THE JOURNAL OF PHYSICAL CHEMISTRY C

Article

pubs.acs.org/JPCC

Vertically Cobalt Nanoplate Arrays Based on One-Step Electrochemical Growth and Their Magnetic Properties

Lixia Xu, Shichao Zhang,* Wenbo Liu, and Zhijia Du

School of Materials Science and Engineering, Beihang University, Beijing, China

Supporting Information

ABSTRACT: A cobalt nanoplate array (Co NPA) directly grown on a copper substrate by the one-step electrodeposition method is synthesized without any template. Most of the nanoplates with a height of ~350 nm and length of up to several micrometers stand vertically on the copper substrate. The as-prepared cobalt nanoplates have the {100} crystal facets as the basal plane. By adjusting the electroplating conditions, the morphology and size of the cobalt nanocrystal can be modulated. Owing to the interesting anisotropic nanostructures, remarkable magnetic anisotropy is obtained on the Co NPA. In addition, the cobalt nanoplates are demonstrated to show enhanced magnetic properties compared with other cobalt nanostructures.

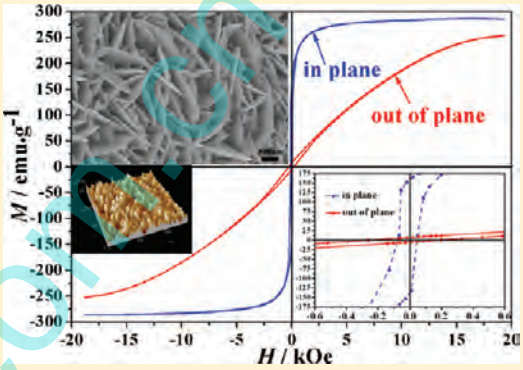

INTRODUCTION

In recent years, magnetic nanomaterials have attracted conciderable interest due to their novel properties and many applications in electronic, optical, catalytic, magnetic, and other areas.[1−4] Compared to other magnetic metals, cobalt, which has one of the highest spin imbalances at the Fermi level, has received increasing attention. To achieve better performance in special utilities, the anisotropy of the magnetic nanomaterials must be well controlled.[5,6] To improve the magnetic anisotropy of the materials, much attention has been paid to assembling low-dimensional cobalt nanostructures into three-dimensional (3D) complex architectures.[7] Up to now, the preparation of shape-anisotropic cobalt nanocrystals has mainly been achieved in a solution phase containing a surfactant by chemical methods. Cobalt nanocrystals with modified intrinsic properties, including nanorods,[8] nanodiscs,[9] nanocones,[10] nanoplatelets,[11,12] wires,[13] cubic nanoskeletons,[14] octahedron-like Co nanocrystals,[15] and chains of hollow cobalt mesospheres,[16] have been prepared.

To develop functional nanodevices, nanostructures are required to be constructed or assembled on substrates. Though many efforts have been made to understand and control the surface growth of nanoparticles, the preparation of nanoparticles on substrates with well-defined shape and size is still a challenge for nanostructure construction. Electrochemistry is an efficient method for directly producing and patterning metal nanocrystals on conducting substrates. Cobalt crystals have been deposited on substrates such as stainless steel, vitreous carbon, and copper, in electrochemical ways from different electrolytic baths containing chloride, sulfate, or thiocyanate aqueous solutions.[17−20]

In this paper, we report a facile galvanostatic synthetic method for a cobalt nanoplate array (Co NPA) by adding ammonium citrate dibasic ($(NH_4)_2C_6H_6O_7$) as a modifying agent. The experimental results show that most of the prepared nanoplates stand vertically on the substrate and there are many edges or controlled nanogaps in the array. Meanwhile, the growth conditions, phase structures, and magnetic properties of the 3D Co NPA were systematically studied.

EXPERIMENTAL SECTION

All of the chemicals were analytical grade reagents obtained from commercial sources and were used without further purification. In this work a (99.5%) 1 cm × 2 cm Cu substrate served as the working electrode in a three-electrode electrodeposition system with a saturated calomel electrode (SCE) as the reference electrode and a 5.0 cm × 3.5 cm titanium plate as the counter electrode. The photoresist was used by defining the area of the Cu plates deposited. Prior to the electrodeposition, the substrates were mechanically polished, rinsed with distilled water, dipped into a hydrochloric aqueous solution (10%) (60 s) to remove the native oxide, and then rinsed again with distilled water. The electrolyte was comprised of 0.1 M $CoSO_4·7H_2O$, 1 M H_3BO_3, and 0.5 M $(NH_4)_2C_6H_6O_7$. The galvanostatic technique was carried out under appropriate current control.

The morphology of the cobalt crystals was investigated using field-emission scanning electron microscopy (FESEM; Hitachi S-4800) with an energy-dispersive X-ray (EDX) analyzer. Microstructural characterization of the products was accomplished using X-ray diffraction (XRD; Rigaku D/Max-2400) with Cu Kα radiation (λ = 1.5418 Å) at a step rate of 0.1 deg/s

Received: November 19, 2011
Revised: December 26, 2011
Published: January 3, 2012

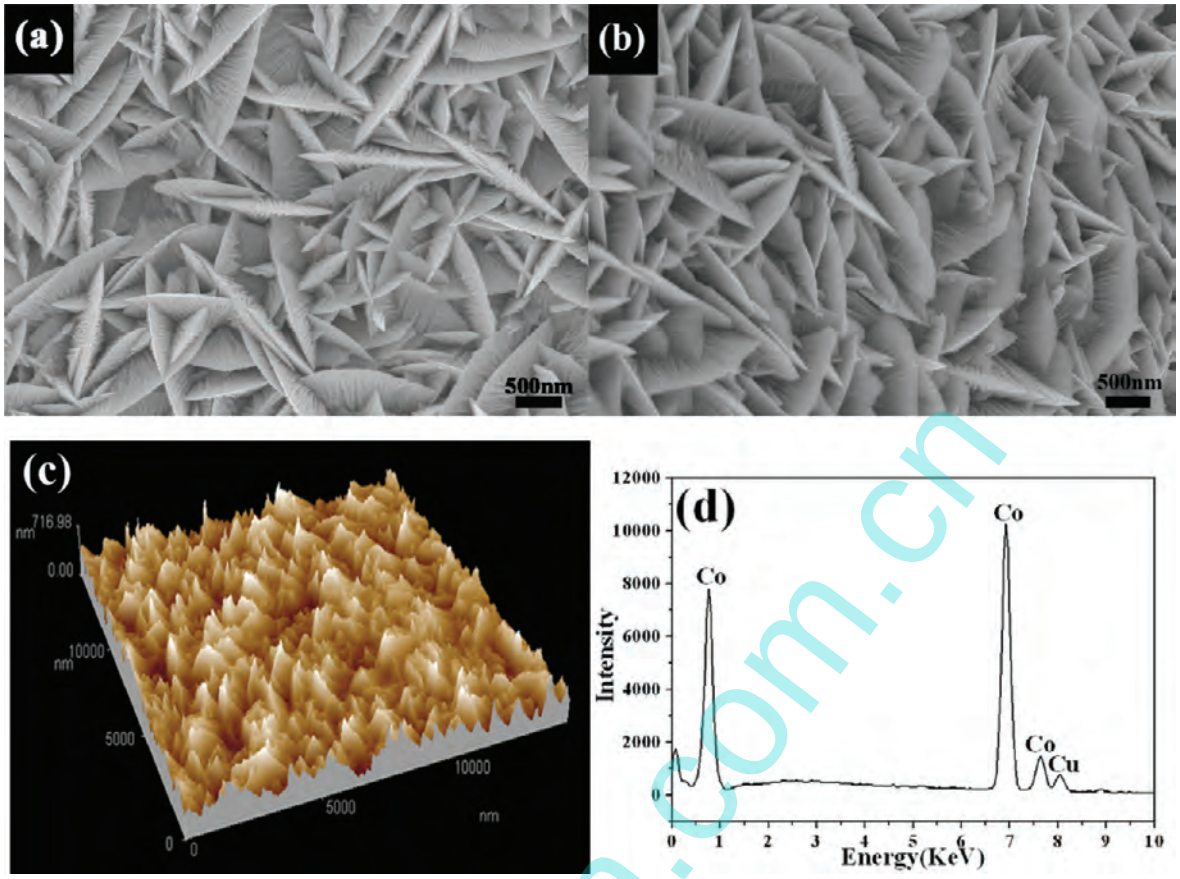

Figure 1. (a) SEM image of the as-synthesized cobalt nanoplates at 65 °C for 1200 s. (b) SEM image of the nanoplates in (a) at 45°. (c) Tapping mode AFM image of the cobalt nanoplates. (d) EDS pattern of the cobalt nanoplates.

in the 2θ range of 40−100°. The topography of the deposits was investigated using a Nanoscope Dimension CSPM5500 atomic force microscope working in tapping mode. Considering the strong binding force between the cobalt film and cobalt plates, transmission electron microscopy (TEM; JEM-2100F) samples were prepared by scraping a little powder from the electrode and dispersing it in alcohol by ultrasonic treatment. Sebsequently, the suspension was dropped onto a holey carbon film supported on a copper grid. All electrochemical measurements were performed in a conventional three-electrode cell at ambient temperature (42−87 °C) using an electrochemical workstation (PARSTAT 2273). The magnetic moment **M** was measured as a function of the applied magnetic field ranging from −20 to +20 kOe. Measurements were conducted using a PPMS-14T (Quantum Design).

RESULTS AND DISCUSSION

The Co NPAs prepared from the electrolyte with 0.1 M $CoSO_4$, 0.5 M $(NH_4)_2C_6H_6O_7$, and 1 M H_3BO_3 by the galvanostatic technique with the apparent current density strictly controlled to 1.25A/dm^2 are shown in Figure 1a,b (taken at an inclination angle of 45°). As can be seen from Figure 1a,b, most of the cobalt nanoplates orient themselves perpendicular to the copper substrate. It should be mentioned that the thickness of the cobalt nanoplates is not unifom; the top of the nanoplates is sharp with a thickness of ∼30 nm, while the base is much thicker (∼150 nm). The topography of the products obtained by atomic force microscopy (AFM) is shown in Figure 1c. It indicates that the average height of the nanoplates is around 400 nm. The energy-dispersive spectrometry (EDS) analysis (Figure 1d) shows that the sample is essentially pure cobalt.

The XRD pattern of the sample is shown in Figure 2a. No characteristic peaks due to the impurities of cobalt oxides or hydroxide were detected, indicating that Co crystals with high purity were obtained by our electrochemical deposition strategy. The characteristic peaks of the as-prepared products arise at 2θ = 41.7°, 44.5°, 47.5°, 75.9°, 84.2°, 92.5°, and 94.7°, which have been assigned to hexagonal close-packed (hcp) Co (100), (002), (101), (110), (103), (112), and (201) planes, respectively (JCPDS no. 05-0727). Moreover, the (100) diffraction gives a higher intensity than is expected, which indicates that the crystallites are abundant in (100) facets and thus their (100) planes tend to be preferentially oriented. Apart from the peaks assigned to hcp cobalt, there are some peaks that can be indexed as face-centered cubic (fcc) cobalt. The characteristic peaks arise at 2θ = 44.2°, 75.9°, and 92.5°, which have been assigned to fcc (111), (220), and (311) planes indexed as fcc Co (JCPDS no. 15-0806). This suggests that the hcp and fcc phases of cobalt nanocrystal coexist in the products. We consider that besides the cobalt nanoplates there may exist another kind of morphology of cobalt nanocrystals at the bottom and thus deduce that the two kinds of crystal structures (hcp and fcc) may correspond to the two kinds of morphologies of cobalt nanocrystals, respectively. Figure 2 b shows the typical TEM image of a single cobalt nanoplate with perfect platelike shape. The structural orientation of an individual nanoplate was investigated by HRTEM, as shown

dx.doi.org/10.1021/jp2111583 | J. Phys. Chem. C 2012, 116, 2801−2806

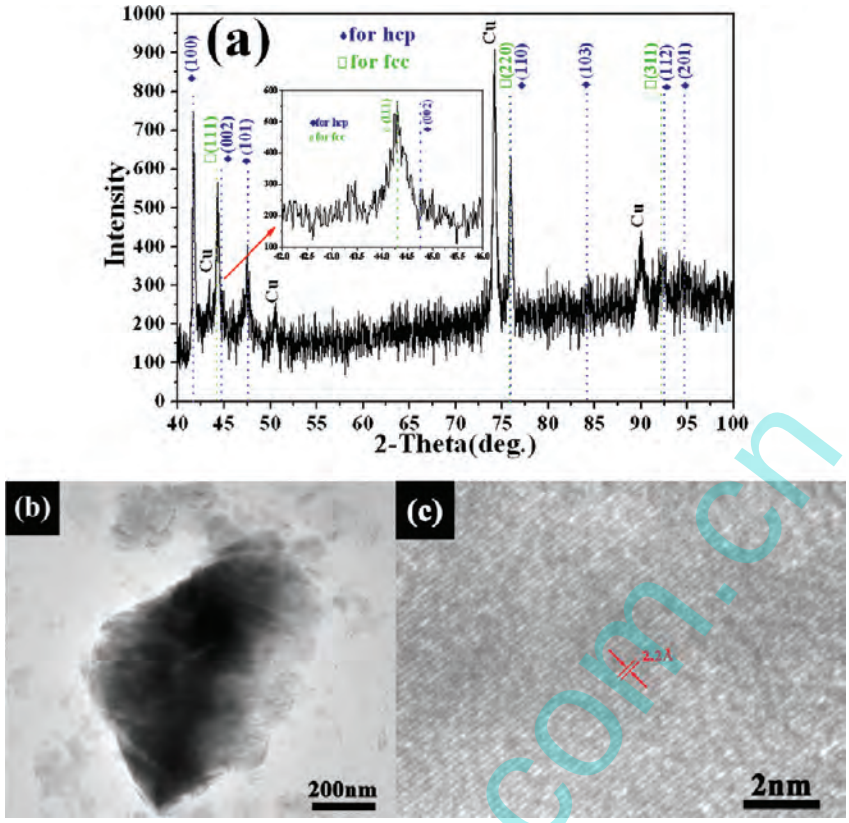

Figure 2. (a) XRD patterns of cobalt nanoplates. (b) TEM image of the cobalt nanoplates. (c) Typical HRTEM image corresponding to (b).

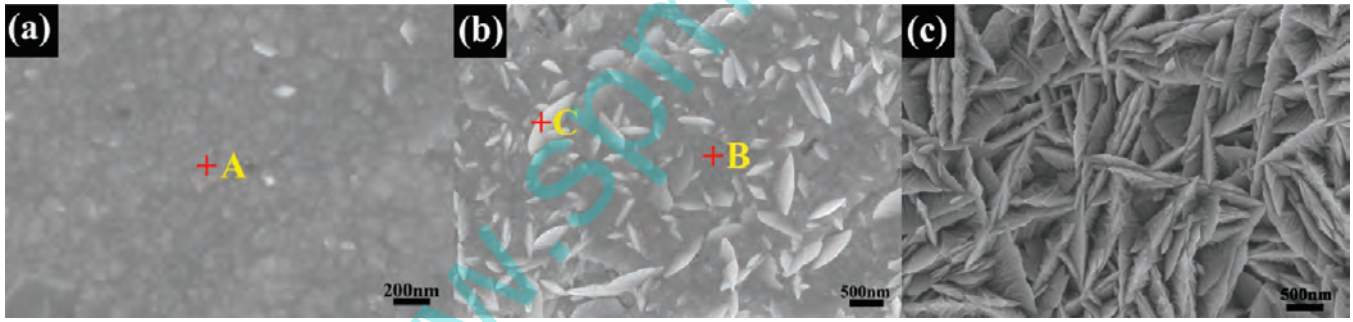

Figure 3. SEM images of the cobalt nanoparticles prepared for different times: (a) 120 s, (b) 360 s, (c) 3600 s.

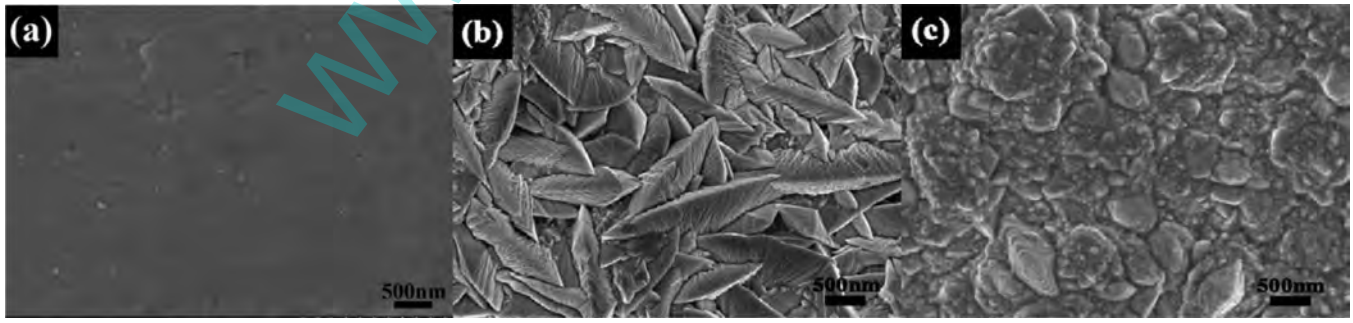

Figure 4. SEM images of the cobalt nanoparticles prepared under different current densities: (a) 0.25 A/dm^2, (b) 4 A/dm^2, (c) 4.5 A/dm^2.

in Figure 2c. The image of the {100} cobalt lattice planes with a space of 0.22 nm between the neighboring lattice planes, in agreement with the *d*100 space of hcp Co, with no disruption of the lattice planes, indicates that the nanoplate is a perfect single crystal.

To prove the existence of another kind of morphology of cobalt nanocrystals, the morphology evolution of nanoplates against time was studied (Figure 3). After 120 s of deposition, only a layer of cobalt film appeared (Figure 3a). With the deposition time increasing to 360 s, the final product was

dx.doi.org/10.1021/jp2111583 | J. Phys. Chem. C 2012, 116, 2801–2806

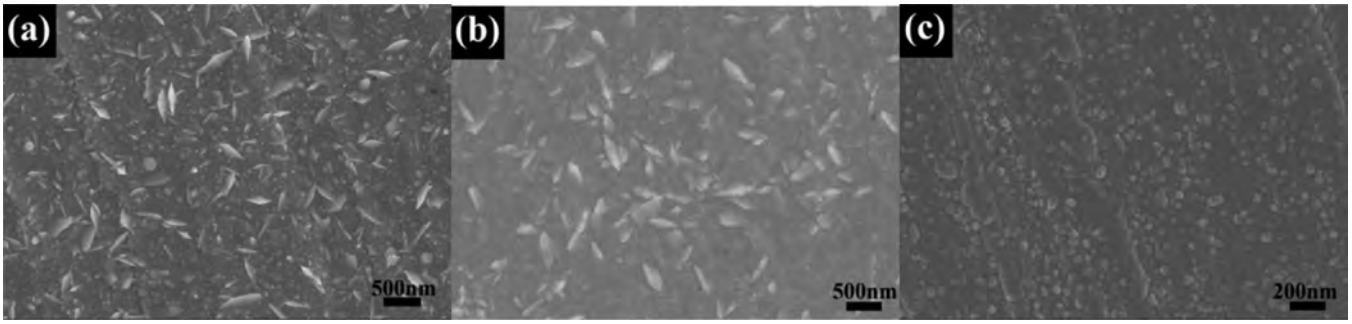

Figure 5. SEM images of the cobalt nanoparticles prepared under different temperatures: (a) 25 °C, (b) 85 °C, (c) 95 °C.

dominated by a cobalt film together with only a few narrow nanoplates with a length of 500 nm (Figure 3b). The EDS details corresponding to points A−C) of Figure 3a,b are shown in Figure S1 (Supporting Information). If the deposition time was further increased to 3600 s, the vertically standing cobalt nanoplates were denser in distribution and ever-increased in size (Figure 3c), but the morphology remained stable. On the basis of the above analysis, the formation of Co NPA could be explained from the point of view below. At the prophase of the deposition, a layer of cobalt film is deposited on the substrate. The ammonium and citrate ions preferentially adsorb on certain orientations, thereby retarding the growth rate of cobalt along certain directions while the surface without surfactant adsorption grows preferentially.[21] In addition, the oriented electric field between the working electrode and the counter electrode assists the vertical growth of nanoplates, since the electric line force was perpendicular to the substrate.[22,23]

The growth rate of the crystal plays an important role in the formation of anisotropic nanocrystals. One of the advantages of the electrodeposition is that the rate of the crystal growth can be controlled by adopting different current densities. The morphology evolution of cobalt nanocrystals on a copper substrate as a function of the current density is clearly seen in Figure 4. Under a current density of 0.25 A/dm^2, only a smooth cobalt film was generated in Figure 4a. Vertical cobalt nanoplates could be prepared only under a current density ranging from 0.75 to 2.75 A/dm^2 (Figure S2, Supporting Information). When the current density increased to 3.5 A/dm^2, it showed trapeziform nanoplates standing on the substrate (Figure 4b). However, the thickness and length obviously increased from 0.75 to 3.5 A/dm^2 . When the current density reached 4.5 A/dm^2, the cobalt nanoplates became irregular bulk particles (Figure 4c). This is because the cobalt crystals are prone to grow at almost the same speed along different crystal orientations under a high current density, namely, isotropic growth of cobalt nanocrystals.

It can be seen from the XRD patterns of the samples corresponding to Figures 1a and Figure 4b,c (Figure S3, Supporting Information) that the intensity of the characteristic peaks of (100), one plane of hcp, decrease as the current density increases, while the intensity of the characteristic peaks of (111), one plane of fcc, increase as the current density increases. This indicates that an electrodeposited cobalt nanocrystal favors the hcp structure at lower negative current densities, the fcc structure at higher negative current densities, and mixed phases of fcc and hcp between them. The present results demonstrate that different crystal structures of cobalt crystals can be obtained through simply changing the deposition current density.

In an electrochemical deposition route, temperature has a direct influence on the formation of the crystal nuclei and growth by affecting the diffusion of primary particles in the electrolyte and the adsorption on the crystal surface, thus affecting the morphology and crystal structures of the products. At 25 °C (Figure 5a) and 85 °C (Figure 5b), narrow cobalt nanoplates started to emerge. Co NPAs can only be found growing orderly at temperatures ranging from 45 to 75 °C (Figure S4, Supporting Information). When the temperature is increased to 95 °C (Figure 5c), the formation of particles is brought about. It is generally recognized that a higher temperature favors growth vertical to the substrates, because with an increase of temperature, the diffusion layer of the adsorptive atom will be thicker, and the roughness of the deposit will be increased. However, if the temperature exceeds a certain limit, the electroplating system will change, resulting in decomposition of the complex.

Complexants have been widely utilized to modify the morphology of metallic nanomaterials prepared by electrodeposition of the corresponding metallic salts. To further investigate the influence of complexants, comparison experiments without ammonium or citrate ions were performed. The morphology of the as-obtained products (Figure S5, Supporting Information) is similar to that of the products with both ammonium and citrate ions ($(NH_4)_2C_6H_6O_7$) (Figure 1a) but much thicker, lower, and sparser. This implies that ammonium and citrate ions have a great effect on promotion of the orientation growth of the cobalt nanoparticles. The X-ray diffraction pattern of the samples (Figure S6, Supporting Information) shows that the characteristic peaks of two kinds of electrodeposited samples aforementioned arise at almost the same positions, which indicates that they have almost the same crystal structure.

The hysteresis loops with the field perpendicular (out-of-plane) and parallel (in-plane) to the Cu substrate for the cobalt nanoplates corresponding to Figure 1a are shown in Figure 6a. The values of squareness SQ (ratio of remanence to saturation magnetization, $\mathbf{M}_r/\mathbf{M}_s$) are $SQ_{\parallel}$ = 0.559 and $SQ_{\perp}$ = 0.0306, which indicates that the easy magnetization axis is parallel to the substrate plane and hence perpendicular to the cobalt nanoplate axis. The coercivity of the Co NPAs is ∼285.6 and ∼46.1 Oe (1 Oe = $103/4\pi$ A m^{-1}) for $\mathbf{H}_{\perp}$ and $\mathbf{H}_{\parallel}$, respectively. It is obvious that the loop measured in $\mathbf{H}_{\perp}$ has a larger coercivity (∼285.6 Oe) in comparison to that measured in $\mathbf{H}_{\parallel}$ (∼46.1 Oe), indicating a remarkable magnetic anisotropy. Compared with the coercivity value of the bulk one (a few tens of oersteds at room temperature) and the similar microstructures reported previously, the cobalt nanoplates with a magnetic field applied perpendicular to the copper substrate

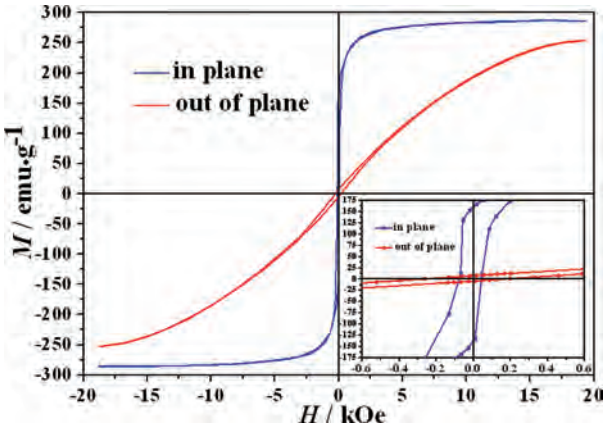

Figure 6. Magnetic hysteresis loop of the Co sample.

exhibit a distinct enhanced coercive force, which is attributed to their special 3D structure. Figure 7a presents the relationship of H_c values versus temperature when the applied field is parallel and perpendicular to the substrate. It clearly shows that H_c is significantly decreased as the temperature increases. Figure 7b illustrates the typical angular dependence of the coercivity and squareness for Co NPAs, where θ is the angle between the substrate and the applied field during measurement. It can be observed that the maximum coercivity occurs at 75° while the maximum squareness occurs when the applied field is parallel to the substrate. Also, the squareness decreases as θ increases. These results are consistent with the general trend of the relationship between the squareness and θ.

CONCLUSIONS

In summary, hcp Co NPAs standing vertically on the substrate were synthesized via a facile complexant-assisted galvanostatic method. Ammonium citrate dibasic can be used to effectively assist the formation of shape-anisotropic cobalt nanocrystals. By adjusting the electroplating conditions, the size and shape of the cobalt nanoplates can be controlled. A discernible difference is observed between the hysteresis loops when **H** is applied parallel ($H_{||}$ = 27.1 Oe) and perpendicular ($H_{\perp}$ = 285.6 Oe) to the copper substrate. A ferromagnetic nature with a significantly enhanced magnetic coercivity ($H_{\perp}$ = 285.6 Oe) can be exhibited due to the anisotropic shape and the hcp crystal structure. This simple strategy also can be easily extended to fabricate other metal nanoplate arrays on the substrate, leading to a broad promising application in many fields.

ASSOCIATED CONTENT

Supporting Information

EDS patterns of the cobalt nanoplates corresponding to points A–C in Figure 3, SEM images of the cobalt nanoplates prepared under different current densities and different temperatures and of the platelike Co nanocrystals deposited without ammonium and citrate ions, and XRD patterns of cobalt plates deposited under different currents and of the Co nanocrystals deposited with and without ammonium and citrate ions. This material is available free of charge via the Internet at http://pubs.acs.org.

AUTHOR INFORMATION

Corresponding Author

*E-mail: xulixiabuaa@163.com.

ACKNOWLEDGMENTS

This work was supported by the National Natural Science Foundation of China (Grants 50954005 and 51074011), the National Basic Research Program of China (Grant 2007CB936502), and the National 863 Program (Grants 2006AA03Z230 and 2008AA03Z208).

REFERENCES

(1) Legrand, J.; Ngo, A. T.; Petit, C.; Pileni, M. P. *Adv. Mater.* **2001**, *13*, 58–+.
(2) Legrand, J.; Petit, C.; Pileni, M. P. *J. Phys. Chem. B* **2001**, *105*, 5643–5646.
(3) Tzitzios, V.; Niarchos, D.; Gjoka, M.; Boukos, N.; Petridis, D. *J. Am. Chem. Soc.* **2005**, *127*, 13756–13757.
(4) Rafailovic, L. D.; Karnthaler, H. P.; Trisovic, T.; Minic, D. M. *Mater. Chem. Phys.* **2010**, *120*, 409–416.
(5) Puntes, V. F.; Krishnan, K. M.; Alivisatos, A. P. *Science* **2001**, *291*, 2115–2117.
(6) Li, M.; Hang, T.; Fei, Q.; Mao, D. *Nanotechnology* **2008**, 19.
(7) Soumare, Y.; Garcia, C.; Maurer, T.; Chaboussant, G.; Ott, F.; Fievet, F.; Piquemal, J. Y.; Viau, G. *Adv. Funct. Mater.* **2009**, *19*, 1971–1977.
(8) Srikala, D.; Singh, V. N.; Banerjee, A.; Mehta, B. R.; Patnaik, S. *J. Nanosci. Nanotechnol.* **2009**, *9*, 5627–5632.
(9) Hang, T.; Hu, A. M.; Li, M.; Mao, D. L. *CrystEngComm* **2010**, *12*, 2799–2802.

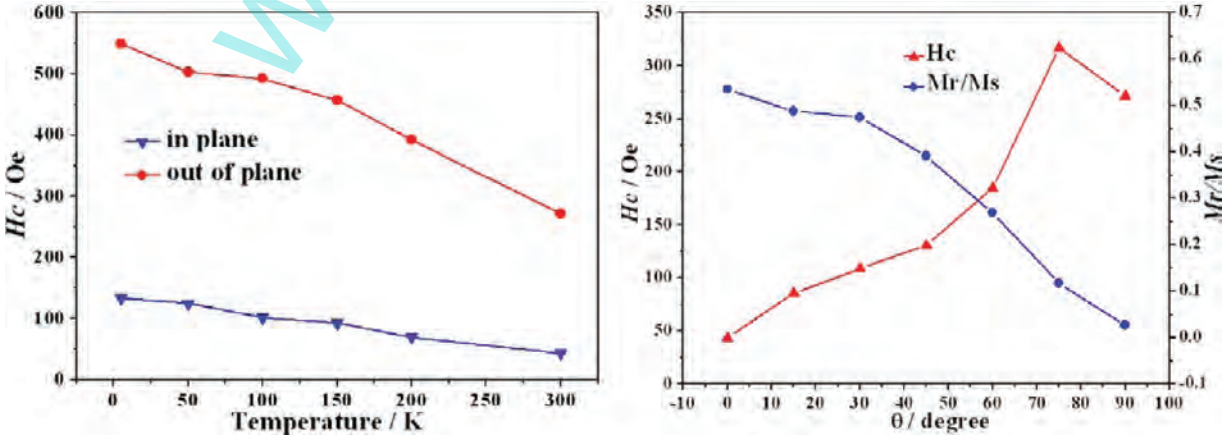

Figure 7. (a) Coercive field against temperature. (b) Angular dependence of coercivity and squareness for the cobalt nanoplates.

dx.doi.org/10.1021/jp2111583 | *J. Phys. Chem. C* 2012, 116, 2801–2806

(10) Zhu, Y.; Yang, Q.; Zheng, H.; Yu, W.; Qian, Y. *Mater. Chem. Phys.* **2005**, *91*, 293−297.
(11) Shin, N. C.; Lee, Y.-H.; Shin, Y. H.; Kim, J.; Lee, Y.-W. *Mater. Chem. Phys.* **2010**, *124*, 140−144.
(12) Xie, B. Q.; Qian, Y. T.; Zhang, S. Y.; Fu, S. Q.; Yu, W. C. *Eur. J. Inorg. Chem.* **2006**, 2454−2459.
(13) Wang, X.; Fu, H. B.; Peng, A. D.; Zhai, T. Y.; Ma, Y.; Yuan, F. L.; Yao, J. N. *Adv. Mater.* **2009**, *21*, 1636−+.
(14) Wang, X.; Yuan, F. L.; Hu, P.; Yu, L. J.; Bai, L. Y. *J. Phys. Chem. C* **2008**, *112*, 8773−8778.
(15) Guo, L.; Liang, F.; Wen, X. G.; Yang, S. H.; He, L.; Zheng, W. Z.; Chen, C. P.; Zhong, Q. P. *Adv. Funct. Mater.* **2007**, *17*, 425−430.
(16) Rios-Reyes, C. H.; Granados-Neri, M.; Mendoza-Huizar, L. H. *Quim. Nova* **2009**, *32*, 2382−2386.
(17) Harti, H.; Bubendorff, J. L.; Florentin, A.; Pirri, C.; Ebothe, J. *J. Cryst. Growth* **2011**, *319*, 79−87.
(18) Karami, H.; Mohammadzadeh, E. *Int. J. Electrochem. Sci.* **2010**, *5*, 1032−1045.
(19) Grujicic, D.; Pesic, B. *Electrochim. Acta* **2004**, *49*, 4719−4732.
(20) Yan, F.; Luo, Z. X.; Zhou, X. F.; Yao, H. N. *Mater. Chem. Phys.* **2008**, *107*, 91−95.
(21) Bao, Z. L.; Kavanagh, K. L. *J. Cryst. Growth* **2006**, *287*, 514−517.
(22) Jia, F. L.; Wong, K. W.; Du, R. X. *Electrochem. Commun.* **2009**, *11*, 519−521.
(23) Jia, F. L.; Wong, K. W.; Zhang, L. Z. *J. Phys. Chem. C* **2009**, *113*, 7200−7206.